$CDCl_3$, 60 °C): $\delta = -0.71$ (s, 4H, ${}^{a}CH_2$), 3.50 (d, ${}^{3}J(H,H) = 1$ Hz, 4H, ${}^{b}CH$), 3.97 (s, 8H, ${}^{d}CH_2$), 4.87–5.00 (m, 48H, ${}^{g}CH_2 + {}^{j}CH_2$), 5.65 (t, ${}^{3}J(H,H) = 1$ Hz, 2H, ${}^{c}CH$), 6.30 (d, 8H, ${}^{e}CH$), 6.44 (t, ${}^{3}J(H,H) = 1$ Hz, 4H, ${}^{f}CH$), 6.54 (t, ${}^{3}J(H,H) = 1$ Hz, 8H, ${}^{i}CH$), 6.65 (d, ${}^{3}J(H,H) = 1$ Hz, 16H, ${}^{h}CH$), 7.24–7.38 (m, 80H, ${}^{k}C_6H_5$), 8.12–8.14 (m, 8H, ${}^{l}CH$), 9.49–9.52 (m, 8H, ${}^{m}CH$); UV/Vis (toluene): λ_{max} (ε) = 680 nm (250000), FAB-MS: m/z: 3726 [M^+].

Crystal structure analysis of **2**: $C_{130}H_{102}N_8O_{14}Si$, $M_r = 2028.37$, green prismatic crystal, crystal dimensions 0.07 × 0.3 × 0.4 mm, triclinic, space group $P\bar{1}$ (no. 2); $a = 14.079(3)$, $b = 16.291(5)$, $c = 12.710(3)$ Å, $\alpha = 103.62(2)$, $\beta = 109.30(2)$, $\gamma = 71.83(2)°$, $V = 2585(1)$ Å^3, $Z = 1$, $\rho_{calcd} = 1.303$ g cm^{-3}, $\mu = 0.9$ cm^{-1}; Rigaku AFC5R diffractometer, monochromatized $Mo_{K\alpha}$ radiation ($\lambda = 0.71069$ Å), 20 °C, $\omega - 2\theta$ scan mode; $2\theta_{max} = 50.1°$; 9709 measured reflections, 9175 unique reflections ($R_{int} = 0.102$), 691 parameters refined, 4023 reflections included in the refinement. Lorentzian, polarization, and absorption corrections were carried out (transmission factors = 0.9331–1.0000; $\mu = 0.9$ cm^{-1}). A decay correction based on a 4.5% decrease in the intensity of three standard reflections was also applied. The structure was determined by direct methods (SHELXS86) and expanded by Fourier techniques (DIRDIF94). The non-hydrogen atoms were refined anisotropically. Hydrogen atoms were included in calculated positions but not refined. Refinement was carried out by full-matrix least-squares methods on 4023 observed reflections ($I > 2.50\sigma(I)$) and 691 variable parameters; $R = 0.067$; $R_w = 0.052$; maximum and minimum peaks on the final Fourier map corresponded to 0.29 and -0.24 e Å^{-3}. Crystallographic data (excluding structure factors) for the structure reported in this paper have been deposited with the Cambridge Crystallographic Data Centre as supplementary publication no. CCDC-100742. Copies of the data can be obtained free of charge on application to CCDC, 12 Union Road, Cambridge CB2 1EZ, UK (fax: (+44) 1223-336-033; e-mail: deposit@ccdc.cam.ac.uk).

Received: October 13, 1997 [Z 11027 IE]
German version: *Angew. Chem.* **1998**, *110*, 1185–1187

Keywords: dendrimers · phthalocyanines · silicon · steric hindrance

---

[1] Recent reviews: a) G. R. Newcombe, C. N. Moorefield, F. Vögtle, *Dendritic Molecules: Concepts, Syntheses and Perspectives*, VCH, Weinheim, **1996**; b) J. M. J. Fréchet, *Science* **1994**, *263*, 1710–1715; c) D. A. Tomalia, *Adv. Mater.* **1994**, *6*, 529–539.

[2] T. Nagasaki, O. Kimura, M. Ukon, I. Hamachi, S. Shinkai, S. Arimori, *J. Chem. Soc. Perkin Trans. 1* **1994**, 75–81.

[3] G. R. Newkome, X. F. Lin, C. D. Weis, *Tetrahedron: Asymmetry* **1991**, *2*, 957–960.

[4] K. Lorenz, D. Hölter, B. Stühn, R. Mülhaupt, H. Fey, *Adv. Mater.* **1996**, *8*, 414.

[5] a) C. Wang, M. R. Bryce, A. S. Batsanov, L. M. Goldenberg, J. A. K. Howard, *J. Mater. Chem.* **1997**, *7*, 1189–1197; b) M. R. Bryce, W. Davenport, A. J. Moore, *Angew. Chem.* **1994**, *106*, 1862–1864; *Angew. Chem. Int. Ed. Engl.* **1994**, *33*, 1761.

[6] C.-F. Shu, H.-M. Shen, *J. Mater. Chem.* **1997**, *7*, 47–52.

[7] a) J. Essberner, F. Vögtle, L. De Cola, V. Balzani, *Chem. Eur. J.* **1997**, *3*, 706–712; b) S. Serroni, A. Juris, M. Venturi, S. Campagna, I. R. Resino, G. Denti, A. Credi, V. Balzani, *J. Chem. Mater.* **1997**, *7*, 1227–1236, and references therein.

[8] a) K. L. Wooley, C. J. Hawker, J. M. J. Fréchet, F. Wudl, G. Srdanov, S. Shi, C. Li, M. Kao, *J. Am. Chem. Soc.* **1993**, *115*, 9836–9837; b) C. J. Hawker, K. L. Wooley, J. M. J. Fréchet, *J. Chem. Soc. Chem. Commun.* **1994**, 925–926; c) P. J. Dandliker, F. Diederich, M. Gross, C. B. Knobler, A. Louati, E. M. Sanford, *Angew. Chem.* **1994**, *106*, 1821–1823; *Angew. Chem. Int. Ed. Engl.* **1994**, *33*, 1739–1741; d) P. J. Dandliker, F. Diederich, J.-P. Gisselbrecht, A. Louati, M. Gross, *ibid.* **1995**, *107*, 2906–2909; **1995**, *34*, 2725–2728; e) R-H. Jin, T. Aida, S. Inoue, *J. Chem. Soc. Chem. Commun.* **1993**, 1260–1262; f) M. Kimura, K. Nakada, Y. Yamaguchi, K. Hanabusa, H. Shirai, N. Kobayashi, *Chem. Commun.* **1997**, 1215–1216.

[9] a) N. B. McKeown, J. Painter, *J. Mater. Chem.* **1994**, *4*, 1153–1155; b) G. J. Clarkson, B. M. Hassan, D. R. Maloney, N. B. McKeown, *Macromolecules* **1996**, *29*, 1854–1856; c) G. J. Clarkson, A. Cook, N. B. McKeown, K. E. Treacher, Z. Ali-Adib, *ibid.* **1996**, *29*, 913–917; d) K. E. Treacher, G. J. Clarkson, N. B. McKeown, *Liq. Cryst.* **1995**, *19*, 887–889; e) K. E. Treacher, G. J. Clarkson, Z. Ali-Adib, N. B. McKeown, *Chem. Commun.* **1996**, 73–75.

[10] N. B. McKeown, *Phthalocyanine Materials: Synthesis, Structure and Function*, Cambridge University Press, Cambridge, in press.

[11] H. S. Nalwa, J. S. Shirk in *Phthalocyanines: Properties and Applications, Vol. 4* (Eds.: C. C. Leznoff, A. B. P. Lever), VCH, New York, **1996**, pp. 83–181, and references therein.

[12] a) W. J. Schutte, M. Sluytersrehbach, J. H. Sluyters, *J. Phys. Chem.* **1993**, *97*, 6069–6073; b) M. Fujiki, H. Tabei, T. Kurihara, *ibid.* **1988**, *92*, 1281–1285.

[13] a) C. J. Hawker, J. M. J. Fréchet, *J. Chem. Soc. Chem. Commun.* **1990**, 1010–1013; b) C. J. Hawker, J. M. J. Fréchet, *J. Am. Chem. Soc.* **1990**, *112*, 7638–7647; c) K. L. Wooley, C. J. Hawker, J. M. J. Fréchet, *ibid.* **1991**, *113*, 4252–4261.

[14] R. D. George, A. W. Snow, *Chem. Mater.* **1994**, *6*, 1587–1588.

[15] M. Emmelius, G. Pawlowski, H. W. Vollmann, *Angew. Chem.* **1989**, *101*, 1475–1502; *Angew. Chem. Int. Ed. Engl.* **1989**, *28*, 1445–1470.

[16] a) R. D. Joyner, M. E. Kenney, *Inorg. Chem.* **1962**, *1*, 236–238; b) *J. Org. Chem.* **1963**, *28*, 3379–3381; c) M. K. Lowery, A. J. Starshak, J. N. Esposito, P. C. Krueger, M. E. Kenney, *Inorg. Chem.* **1965**, *4*, 128–129; d) W. E. Ford, M. A. J. Rodgers, L. A. Schechtman, J. R. Sounik, B. D. Rihter, M. E. Kenney, *ibid.* **1992**, *31*, 3371–3377.

[17] S. Hayashida, N. Hayashi, *Chem. Mater.* **1991**, *3*, 92–95.

Determination of the Disordered Structure of $Gd_2Ba_2CaCu_2Ti_3O_{14}$ with Multiple-Edge EXAFS and Powder Diffractograms[**]

Mark T. Weller,* Maria J. Pack, and Norman Binsted

The structures of solids are defined by local and long-range order, both of which must be determined to characterize a material. Systems in which perfect crystalline order does not exist and local structural features are important include superconducting oxides, alloys, zeolites containing entrapped molecular species, ferroelectric materials, materials that exhibit high magnetoresistance, and intercalation compounds. The structures of such materials are often determined by separate analyses of data collected by a variety of techniques, sometimes with conflicting results, or an averaged structure is determined by analysis of diffraction data alone.

The structure of the complex oxide $Gd_2Ba_2CaCu_2Ti_3O_{14}$ was determined by using a combination of extended X-ray absorption fine structure (EXAFS) data for all five of the metals with powder X-ray diffraction data and refined with a single set of coordinates consistent with all the experimental data. This combined analysis approach, illustrated here, is a

---

[*] M. T. Weller, M. J. Pack, N. Binsted
Department of Chemistry
University of Southampton
Southampton SO17 1BJ (UK)
Fax: (+44) 1703-593-592
E-mail: mtw@soton.ac.uk

[**] This research was supported by the EPSRC through grants X46R352 and GR/J27053 and a studentship for M.J.P.

powerful tool for the characterization of solids whose local structural features cannot be determined or are averaged by diffraction methods. Analyses of multiple-edge EXAFS data sets from various materials have been reported previously,[1–3] but these investigations were limited to a few data sets and did not include diffraction data or a single-crystal structural description.

$Gd_2Ba_2CaCu_2Ti_3O_{14}$ was prepared as described previously.[4] This material provides an excellent example for illustrating the potential of multi-data set analysis, as it adopts a superconductorlike structure with multiple perovskite layers, provides several EXAFS data sets, and has significant local disorder which cannot be fully defined by means of diffraction data alone. The EXAFS spectra were measured at the Daresbury Laboratory Synchrotron Radiation source on stations 8.1 and 7.1. Spectra were recorded in transmission mode, except for the data of the calcium K-edge, which were obtained in fluorescence mode with monochromatic radiation from harmonic-rejecting double-crystal monochromators [Si(111) or Si(220)]. In most cases the samples were poly(vinyl alcohol) disks prepared with a known concentration of sample that depended on the total absorption coefficient of the material, the investigated edge, and the detection technique. A thin disk cosisting solely of sample was used for measuring the calcium K-edge. A minimum of four scans were made for each edge, and the collected data were averaged. Powder X-ray diffraction data (XRD) were collected on a Siemens D5000 $\theta - 2\theta$ diffractometer with $Cu_{K\alpha 1}$ radiation ($\lambda = 1.5406$ Å). Data were collected for 15 h with a step size of 0.02°. The background was subtracted from the EXAFS data with the program PAXAS.[5]

The initial structural model was developed on the basis of powder neutron diffraction data and has been described previously along with those of other members of the 22123 layered perovskite series (Figure 1).[4] Two important features of the refined model derived are the mixed occupation of the A sites by cations, which statistically occupy 8- and 12-fold sites above and below the titanium–oxygen triple layers, and distortion of the TiO_6 octahedra. Initially, EXAFS data from the absorption edges of all five cations in $Gd_2Ba_2CaCu_2Ti_3O_{14}$, XRD data, and the previously defined structural model were read into the combined refinement program.[6] Data for the titanium and barium edges were curtailed at modest k values because of overlap with the barium L_{III}- and L_{II}-edges, respectively. The calcium-edge data were also used in a restricted range of k values, since the scattering statistics were poor because of the presence of heavy absorbing elements. These reduced data ranges, while unavoidable in this material, are not of such significance for a combined refinement technique, as shell distances beyond a few Ångstrom are also defined by the other EXAFS and XRD data. Scattering phase shifts were calculated for each atom in the structure by using ab initio muffin potentials calculated for clusters consisting of two types of atoms. The muffin radii were adjusted so that the charge on the Wigner–Seitz sphere was approximately equal to the atomic number; in each case oxygen atoms were assumed to be the nearest neighbors. In the combined refinement, which required a large number of shells for each of the five edges to simulate the major features of the relative modulation $\chi(k)$ of the absorption coefficients (k is the contribution of the wave vector of the photoelectron), the EXAFS Debye–Waller factors were calculated by using a very simple model (see below). Owing to the different treatments of thermal motion in the XRD and EXAFS methods, the combined analysis program uses two separate descriptions of thermal parameters.[6]

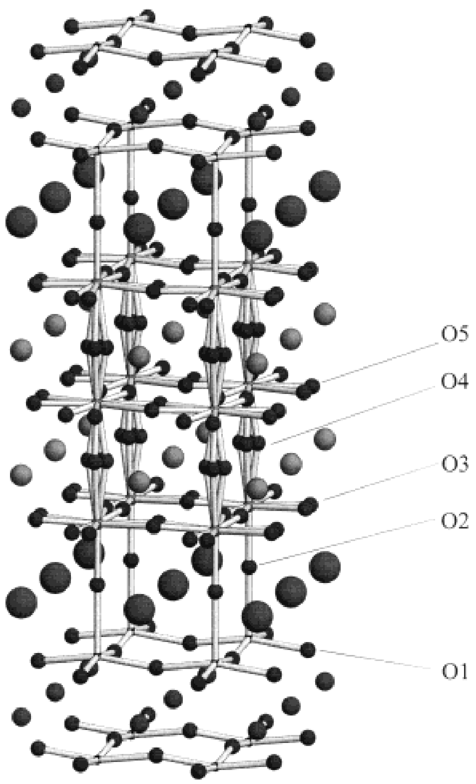

Figure 1. Structure of $Gd_2Ba_2CaCu_2Ti_3O_{14}$. The oxygen atoms are disordered over the sites listed in Table 1. The Cu–O and Ti–O bonds are shown. The Ba atoms are depicted as large, pale gray spheres, the Ca/Gd atoms as medium-sized, dark gray spheres, and Gd atoms that are not bound to O atoms as small, dark spheres.

Initially, the best fit to the XRD data alone was obtained by refining a number of parameters, which included atomic position and temperature factors, peak shape and background parameters, scale factor, and zero offset. After refinement, this structural model differed from that obtained from neutron-diffraction data in having slightly different cell parameters (but comparable within the estimated standard deviations) and slightly shorter average M–O bond lengths. The M–O bond lengths derived from XRD data are generally shorter because the center of electronic density of the oxygen atom is shifted towards the metal center.

A combined refinement with the scattering data was then performed, and the best fit was obtained with XRD parameters (e.g., atomic positions), *Ef* and *AFAC* (*Xe* and *CFAC* for each spectrum), and two new parameters which model all the EXAFS Debye–Waller factors for each involved edgeas a function of the atomic size (Table 1). Thus the total number of parameters that was required in the refinement was decreased, and convergence of each cycle was achieved in a much shorter time.

Table 1. Final parameters from the combined refinement of five EXAFS spectra and a powder X-ray diffractogram (W_{XRD}[g] = 0.2, W_{EXAFS}[g] = 0.8)[a]

Parameter	Refined value	Parameter	Refined value
a [Å]	3.8769(1)	*Bi1* (Gd)[c]	0.8(3)
c [Å]	19.559(1)	*Bi2* (Ba)	1.1(1)
		Bi3 (Ca/Gd)	0.6(3)
Q_r[b]	1.7	*Bi4* (Cu)	0.1(3)
Q_m	2.0	*Bi5*, *Bi6* (Ti)	0.8(1)
		Bi7–*Bi11* (O)	1.0(4)
PZ2	0.1875(2)		
PZ3	0.3972(2)	*Ef*[g]	– 12.00
PZ4	0.0853(2)	*Xe1*, *Xe2*[d, g]	1.8(6)
PZ5	0.3015(14)	*Xe3*	1.0(2)
PZ7	0.0725(8)	*Xe4*	5.4(11)
PZ8	0.2020(19)	*Xe5*, *Xe6*	9.6(7)
PX9	0.061(8)	*Xe7*	7.8(3)
PZ9	0.3048(18)		
PX10	0.075(12)	*AFAC*[g]	0.85
PZ10	0.4050(28)	*CFAC1*, *CFAC2*[d, g]	0.83(2)
PX11	0.122(12)	*CFAC3*	0.99(2)
		CFAC4	0.8[e]
		CFAC5, *CFAC6*	0.57(3)
		CFAC7	0.94(2)
R_{ex}[f]	52.6		
		$R_{\mathrm{wp(XRD)}}$	18.1 %

[a] Atomic positions used to describe the phase $Gd_2Ba_2CaCu_2Ti_3O_{14}$ (space group *P4/mmm*): 1. Gd (1/2,1/2,0); 2. Ba (1/2,1/2,*PZ2*); 3. 0.5 Ca + 0.5 Gd (1/2,1/2,*PZ3*); 4. Cu (0,0,*PZ4*); 5. Ti (0,0,*PZ5*); 6. Ti (0,0,1/2); 7. O1 (0,1/2,*PZ7*); 8. O2 (0,0,*PZ8*); 9. O3 (*PX9*,1/2,*PZ9*) × 1/2; 10. O4 (*PX10*,0,*PZ10*) × 1/4; 11. O5 (*PX11*,1/2,1/2) × 1/2. [b] $A_{in} = Q_m(1/(M_i + M_n)) + Q_r(1/r_{in})$, where A_{in} is the Debye – Waller factor of the *i*th shell in the *n*th spectrum, M_i the atomic mass of the atom in shell *i*, M_n the atomic mass of the central atom in spectrum *n*, and r_{in} the radius of the atom in shell *i* of spectrum *n*. [c] *Bi* is the temperature factor [Å^2] used to fit the diffraction data. [d] For *Xe* and *CFAC* values, the clusters are numbered to represent the central absorber: 1, 2: Gd; 3: Ba; 4: Ca; 5, 6: Ti; 7: Cu. [e] No error is given for *CFAC4* as it was adjusted manually owing to poor-quality data. [f] R_{ex} is the value obtained prior to the inclusion of multiple scattering for copper after variation of all parameters. [g] *Ef* = contribution of the wave vector of the zero photoelectron relative to the origin of *k*; *Xe* = edge-specific *Ef* correction; *AFAC* = amplitude reduction due to many-electron processes; *CFAC* = edge-specific *AFAC*; W_{EXAFS} and W_{XRD} = weightings applied to EXAFS and XRD data sets ($W_{\mathrm{XRD}} + W_{\mathrm{EXAFS}} = 1$).

Once the basic structural model had been refined, individual EXAFS spectra were calculated (i.e., $W_{\mathrm{EXAFS}} = 1.0$) without any further changes in structural positions. Certain features in the EXAFS spectra were consistent with the structural model based on neutron-diffraction data, but R_{ex} at this stage of the refinement was greater than 80. To fit both the EXAFS and XRD data satisfactorily, modifications of the model were required particularly with respect to the positions of the oxygen atoms; this reflects the sensitivity of EXAFS data to the local structure. In the earlier model, the O3 atom on the (0,1/2,*z*) site (Table 1) was not disordered, and O4 was disordered on (*x*,*x*,*z*). For refinement with the EXAFS data, these positions were modified: O3 was moved to a disordered (*x*,1/2,*z*) site, and O4 to a new disordered site (*x*,0,*z*). Moving O3 to the disordered site substantially improved the fit to the data of the barium L_{III}-edge, and the displacement of O4 markedly improved the fits to the calcium- and gadolinium-edge data. Small improvements to the fits to the copper- and titanium-edge data were also achieved. A combined refinement of the data from all five EXAFS edges and the XRD data ($W_{\mathrm{EXAFS}} = 0.8$, $W_{\mathrm{XRD}} = 0.2$) was then carried out with this modified structural model.

Multiple scattering (MS) can make a significant contribution to all EXAFS spectra, but for $Gd_2Ba_2CaCu_2Ti_3O_{14}$ it is only important for the data of the copper and, to a lesser extent, the titanium K-edges owing to the short bond lengths and large M-O-M bond angles of almost 180°. For this reason and because of the considerable increase in computing time required, a full MS calculation was only carried out for the copper-edge data at a late stage of the refinement. Preliminary refinements incorporating multiple scattering for titanium showed minor improvements to the fit for this edge.

The final refined atomic positions for $Gd_2Ba_2CaCu_2Ti_3O_{14}$ are listed in Table 1. Figure 2 illustrates the EXAFS and Fourier transform plots for all five refined data sets. The value of R_{ex} obtained from the refinement of multiple data sets (Table 1) is still relatively high (>50) but significantly improved relative to the initial model. Addition of multiple scattering for copper considerably improved the fit, but because atomic parameters were not refined again, no meaningful new R_{ex} value could be obtained. Another factor contributing to the high combined R_{ex} value is the quality of the calcium K-edge data which does not match that of the other four spectra; this problem in unavoidable due to the presence of the stronger absorbing elements in the compound.

$Gd_2Ba_2CaCu_2Ti_3O_{14}$ is one of a series of ordered quintuple copper – titanium perovskites that are composed of two CuO_2 layers and three TiO_6 octahedra and in which gadolinium, barium, and calcium cations are incorporated between the layers. However, owing to the presence of several structural features, determination of this structure from diffraction data alone[4] leads to an approximate structure with an averaged distribution of the cations and local distortions of the TiO_6 octahedra. Even neutron-diffraction data are relatively insensitive to such features and are unable to distinguish between different similarly disordered structural models owing to strong correlations between positional and thermal factors. The combined refinement reported here allows a more accurate determination of this structure.

Our results have led to the best model so far for the structure of $Gd_2Ba_2CaCu_2Ti_3O_{14}$, and further small improvements could be made by increasing the complexity of the structural model. These would include further disordering of oxygen atoms adjacent to titanium centers and introduction of Ti-O-Ti multiple scattering to improve the fit to the data of the titanium K-edge. The data of the calcium K-edge indicate that the Ca – O bond lengths are shorter than the average Ca/Gd – O distances, and the inclusion of distinct calcium and gadolinium sites may resolve this minor deficiency. However, preliminary (but very computationally intensive) calculations indicate that this more complex model produces only small improvements to the otherwise good fits for multiple data sets (Figure 2). When the new structural model is used in simple Rietveld refinements of X-ray or neutron diffraction data, almost no change in fitting factors was observed. This is evidence for the insensitivity of the diffraction data to the small displacements of the oxygen atoms.

1433-7851/98/3708-1096 $ 17.50+.50/0

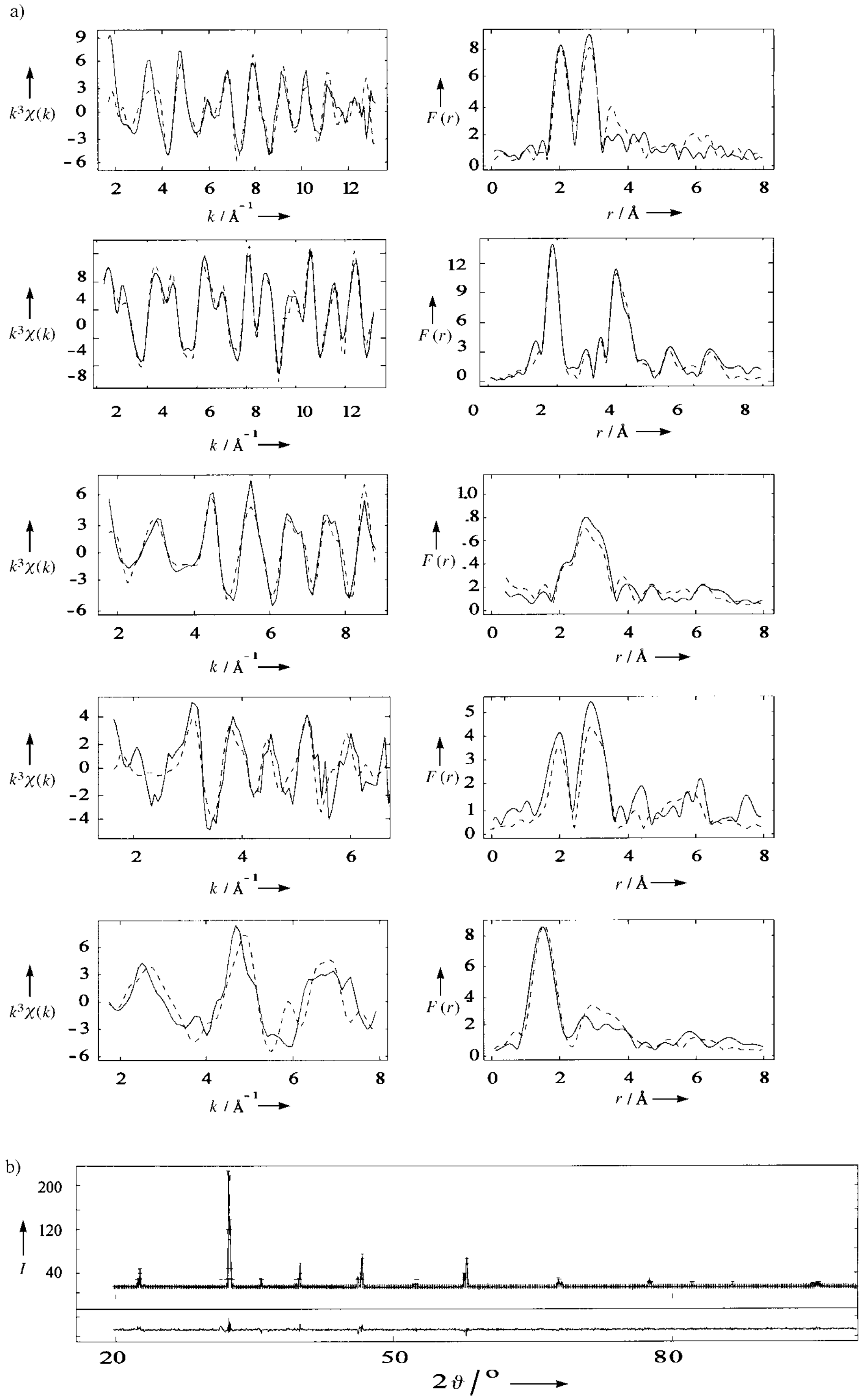

Figure 2. Fits to the EXAFS (a) and powder X-ray diffraction data (b). EXAFS functions and the radial distribution functions $F(r)$ calculated therefrom by Fourier transformation (from top to bottom): Gd (L_{III}), Cu (K), Ba (L_{III}), Ca (K, fluorescence), Ti (K). Experimental data are shown as a dotted line, and calculated values as a solid line. For the diffraction data the experimental data are shown as crosses, the calculated profile as a solid line, and the difference profile as the lower solid line.

We have shown that five sets of EXAFS data and X-ray powder diffraction data can be refined together with a single set of coordinates that define the structure. In addition to showing that such methods for data analysis are possible, we have demonstrated their importance in developing better structural models, particularly for structures in which perfect crystalline order does not exist. This is important for materials such as oxides, in which local environments consist of weakly scattering atoms whose positions may otherwise be very poorly defined. Also in materials such as superconductors, compounds that exhibit high magnetoresistance, alloys, zeolites, ferroelectrics, and intercalates, structure determination by diffraction methods is not definitive. However, by combining a method for determining long-range order with information about the local environment of as many atoms as possible in a refinement of multiple data sets, a better structure elucidation is possible.

Received: October 9, 1997
Revised version: February 9, 1997 [Z11022IE]
German version: *Angew. Chem.* **1998**, *110*, 1193–1196

Keywords: cuprates • EXAFS spectroscopy • structure elucidation

---

[1] A. DiCicco, M.Minicucci, *J. de Physique IV* **1997**, *7C2*(2), 1027.

[2] A. DiCicco, *J. de Physique IV* **1997**, *7C2*(1), 171.

[3] H. H. Zhang, A. Filipponi, A. DiCicco, M. J. Scott, R. H.Holm, B. Hedman, K. O.Hodgson, *J. Am. Chem. Soc* **1997**, *119*, 2470.

[4] M. J. Pack, A. Gormezano, M. T. Weller, *Chem. Mater.* **1997**, *9*, 1547–1553.

[5] N. Binsted, PAXAS (Program for the Analysis of X-ray Absorption Spectra), University of Southampton, **1988.**

[6] N. Binsted, M. J. Pack, M. T. Weller, J. Evans, *J. Am. Chem. Soc.* **1996**, *118*, 10200–10210.